# CHAPTER 2

# SYNTHESIS OF MAGNETIC NANOPARTICLES AND THEIR USE IN THE PREPARATION OF MAGNETIC-MOLECULARLY IMPRINTED SILICAS

## 2.1 Introduction

Molecular imprinting is an efficient technique to generated a 3D cross-linked polymer network with highly selective recognition site for specific template [40]. Typically, molecularly imprinted polymers (MIPs) are synthesized by polymerization reactions involving three main steps (Fig 2.1). First, the self-assembly of functional monomers and templates was allowed to form template-monomer complexes through covalent, non-covalent, or semi-covalent interactions. Then the assembled complexes were fixed into spatial arrangement by the cross-linking polymerization reaction. Finally, the template molecules are removed leaving vacant cavities which are complementary in size, shape and chemical functionality to the template species [41]. These cavities have the ability to selectively rebind the template (Fig. 2.1).

Generally, the molecularly imprinting research has focused on the synthesis of polymeric network using organic acrylic and vinylic monomers (among other functionalities) and a cross-linker (e.g., bis- or trisacrylates, vinyl benzenes, acrylamides, and piperazines) with an initiator like azobisisobutylonitrile (AIBN) [42]. The final polymers are not necessarily porous and the polymerization process often requires organic solvent and high reaction temperature. Moreover, hydrophilic

template molecules that are only soluble in aqueous media are not enable to imprinting in such a manner. This presents obvious limitations for their use in environmental and biological applications. Although some promise has been shown for aqueous based rebinding procedures [43], such results are rare and considerable progress is required to overcome this limitation.

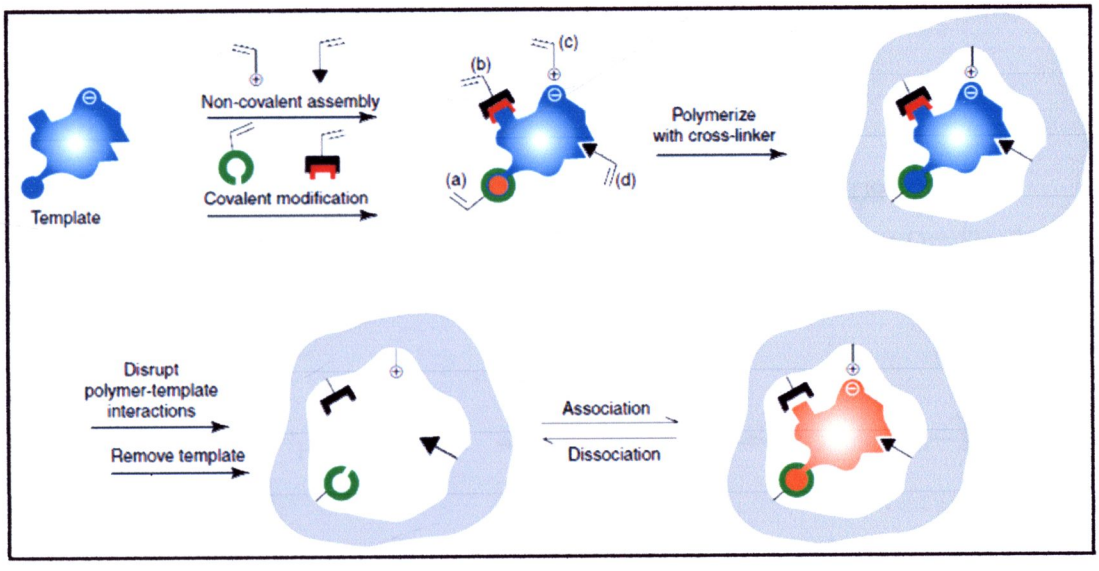


**Figure 2.1** The molecular imprinting process [44].

To overcome the above limitations, sol–gel imprinting can be used as an alternative method to prepare imprint materials. Sol–gels are inorganic (siloxane) based cross-linked polymers formed by the acid or base catalyzed hydrolysis and condensation of a of suitable metal alkoxides [45]. The most widely used precursors to prepare imprint materials for use in chemical analysis applications have been the silicon alkoxides, particularly tetramethoxysilane (TMOS) or tetraethoxysilane

(TEOS). These reagents can be readily hydrolyzed and condensed under relatively mild conditions as depicted in Fig 2.2.

Step 1 : Hydrolysis

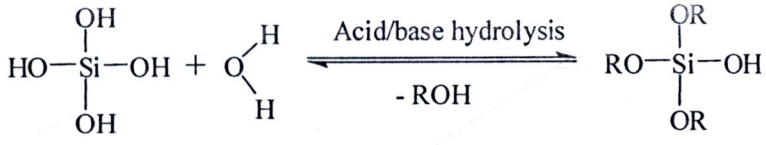


Step 2 : Condensation

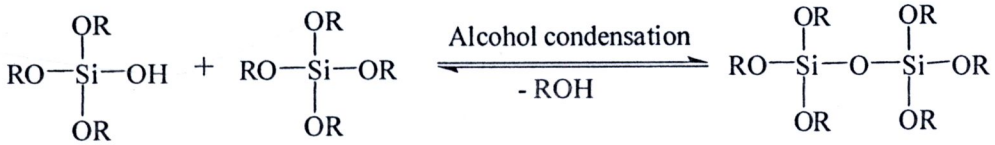


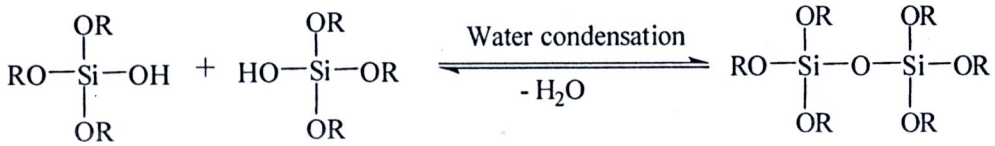


Step 3 : Silica network formation

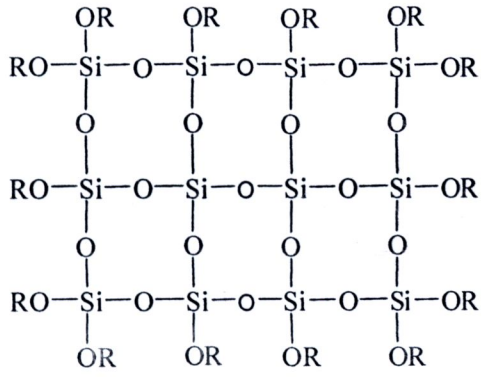

**Figure 2.2** Step-wise description of the sol-gel process [46]

Generally, the synthesis of sol-gel material is a process concerning transition of a system from liquid 'sol' (the colloidal suspension of particles) into solid 'gel'. There are three steps for sol-gel processing [46]; the first method is gelation of colloidal particles, the second is the hydrolysis and polycondensation reactions of alkoxide precursor followed by hypercritical drying, while the third method is similar to the second one: the only difference is the drying process, which takes place at ambient temperatures. The chemical reactions that occur during the formation of sol-gel product occur through a bimolecular nucleophilic substitution at the silicon center ($S_N2$-Si). The hydrolysis reaction under acidic conditions involves protonation of the alkoxide group followed by nucleophilic attack by water to form a penta-coordinate intermediate. The partial positive charge on the alkoxide group confers to it better leaving group character. Under basic conditions, the mechanism is believed to involve the nucleophilic attack on the silicon atom by the hydroxide anion to form a negatively charged penta-coordinated intermediate followed by displacement of an alkoxide anion [47].

Relative to organic-based polymerization schemes, sol-gel processing affords a number of viable advantages for the preparation of imprinted materials. The mild reaction conditions affords an opportunity to incorporate various molecules such a proteins, enzymes, dyes, organic, and organometallic reagents which are not as prone to plasticize into a polysiloxane network. In addition, it can also be readily introduced within a highly crosslinked porous host without problems associated with thermal or chemical decomposition [47]. Specific organic functional groups can be combined

with the inorganic precursor (i.e., TEOS) to introduce specific chemical functionalities into the framework and improve molecular selectivity and specificity [47]. A large diversity of organosilicon derivatives with various functional groups is also commercially available. The representative examples of molecularly imprinted silica (MIS) and their applications are summarized in Table 2.1.

One problem often encounter with imprinted polymers is poor site accessibility of the target molecules because the recognition sites are totally embedded in the polymer matrices. Therefore, the kinetics of the sorption/desorption process is unfavorable and the mass transfer becomes slow. This problem can be overcome by using surface molecular imprinting in which the imprinted materials with binding sites situated at the surface of materials. Many advantages of surface imprinting included high selectivity, more accessible sites, fast mass transfer and binding kinetics [48, 49].

Surface imprinting of silica can be accomplished by combining solid substrate with suitable silane precursors. Various guest molecules like organic, polymeric, biological and metallic materials are readily adsorbed or imprinted using functionalized groups on polysiloxane layer which can then remove by solvent extraction. Thus, surface sol–gel process combined with molecular imprinting technique provides a new platform for various applications.

**Table 2.1** Selected examples of MISs

| Template | Sol-gel system | Application | Ref. |
|---|---|---|---|
| Methyl orange dye | sodium silicate | Dye sorbent | [50] |
| Urease and BSA | APTES, TEOS | Protein sorbent | [48] |
| Uranyl ion ($UO_2^{2+}$) | TMS | Ions sorbent | [51] |
| Cu(II) | TCPTS | Ions sorbent | [52] |
| Yeast cell | MTES or DDTES | Biochemical sensor | [53] |
| Cd(II) | MPTMS | Ions sorbent | [54] |
| Hemoglobin | APTMS, TEOS | Protein separation | [55] |
| L-Histidine | MTMS | Amino acid sensor | [56] |
| PCP | APTES, TEOS | SPE sorbent | [57] |
| BSA | APTMS, TEOS | Protein sensor | [58] |
| Lysozyme | APTES, TEOS | Protein sorbent | [59] |
| Phenyl- and naphthyl functionalized isocyanate | 3-triethoxysilylpropyl-carbamic acid 1-phenyl-ethyl ester or 1-benzyl oxycarbonyl-2-(3-tri ethoxysilyl)propylamino carbonylpyrrolidine | Chromatographic separation | [60] |
| BSA | APTES, OTMS, TEOS | Protein sorbent | [61] |
| Lysozyme , RNase | APTES, TEOS | Chromatographic separation | [62] |
| Luteolin | APTES, TEOS | Sorbent | [63] |

**Table 2.1** Selected examples of MISs (continued)

| Template | Sol-gel system | Application | Ref. |
|---|---|---|---|
| Estazolam | APTES, PTMS, TEOS | SPE sorbent | [64] |
| Pd(II) | MPTMS | Ions sorbent | [65] |
| Bovin hemoglobin (BHb) | APTES | Sensor | [66] |
| 2,4-Dinitro toluene | PTMS, TEOS | SPE sorbent | [67] |
| 2,4-Dichloro phen-oxy acetic acid (2,4-D) | APTES, TEOS | Sorbent | [68] |
| Cd (II) | TCPTES | Ions sorbent | [69] |
| Microcystin-LR (MCT) | APTMS or DPDMS, TEOS | Sensor | [70] |
| Creatinine | TEOS | Sorbent | [71] |

For instance, Li and co-workers reported surface molecular imprinting in combination with sol–gel for protein recognition. The functional biopolymer chitosans (CS) as microsphere were chosen as polysaccharide core for surface imprinting of BSA via covalent linkage. These microspheres were surrounded by aminopropyl trimethoxysilane (APTMS) and TEOS derived hybrid sol–gel silica matrix in aqueous solution at room temperature. After template removal, the protein-imprinted sol–gel surface exhibited a prevalent preference for the template protein in adsorption experiments, as compared with four contrastive proteins. The complementation in

hydrophilicity/ hydrophobicity was a major factor affecting the imprinting formation and template recognition [58].

Recently, Han and co-workers prepared a new molecularly imprinted amino-functionalized silica gel sorbent with binding sites situated at the surface for the template pentachlorophenol (PCP), by a surface imprinting technique in combination with a sol–gel process, and applied it to on-line selective SPE coupled with HPLC for the determination of trace PCP in water samples. PCP is used as a general herbicide in agriculture and as an insecticide for termite control in the preservation of wood [68].

In recent years, magnetic nanoparticles (MNPs) have been applied widely as solid substrate for surface molecularly imprinting technique because of their small size and high surface-to-volume ratio compared with those of the conventional micrometer-size resins or beads. The participation of a magnetic component in the imprinted materials can build a controllable rebinding process and allow magnetic separation to replace the centrifugation and filtration step [72]. When MIS was modified on surface of MNPs, the adsorption can be achieved by dispersing them in solution, and they are then easily separated from the matrix by applying an external magnet.

Jin and co-workers developed a superparamagnetic core-shell molecular imprinting microspheres (MCSIMs) using magnetic particles with 350 nm diameter as solid substrate. Phenylephrine (Phen) was use as a template. APTMS and TEOS were used as silane monomer and cross-linker, respectively. The synthesized MCSIMs have a remarkable affinity to Phen over that of structurally related molecules including

dopamine, epinephrine, phenylalanine and tyrosine. When MCSIMs were applied as amperometric sensor, they also showed high sensitivity, selectivity, reproducibility with long term stability for Phen [73].

In another example, Wang and co-workers presented the synthesis of MIS coated on nanocomposite of magnetic particles for estrone recognition via semi-covalent imprinting technique. In this protocol, the estrone–silica monomer complex (EstSi) was synthesized by the reaction of 3-(triethoxysilyl)propyl isocyanate with estrone, where the template was linked to the silica coating on the iron oxide core via a thermally reversible bond. The removal of the template by a simple thermal reaction produced specific estrone recognition sites on the surface of silica shell. The resulting estrone-imprinted silica coating magnetic hybrid nanoparticles exhibit a much higher specific recognition and saturation magnetization [74].

In this study, surface modified MNPs will be used as a core for surface imprinting by sol-gel method. Main concern are: (i) synthesis of MNPs and modification of MNPs with APTES to obtain aminopropyl magnetic silicas (ii) preparation of magnetic-molecularly imprinted silicas (M-MISs) and evaluation of their binding characteristic.

## 2.2 Experimentals

### 2.2.1 Chemicals

Ammonium solution ($NH_4OH$), $NH_5O$, assay 30%, Carlo Erba, Italy

3-Aminopyridine (3-APY), $C_5H_6N_2$, assay 98%, Fluka, Switzerland

3-Aminopropyltriethoxysilane (APTES), $C_9H_{23}NO_3Si$, assay 98%, Sigma–Aldrich, Germany

Benzoic acid (BZA), $C_7H_6O_2$, assay 98%, Scharlau, Spain

2-Chloronicotinic acid (C-NA), $C_6H_5ClNO_2$, assay 98%, Fluka, Switzerland

Ferric chloride ($FeCl_3 \cdot 6H_2O$), assay 97%, Carlo Erba, Italy

Iron(II) sulphate ($FeSO_4 \cdot 7H_2O$), assay 99%, POCH, Poland

Nicotinamide (NAM), $C_6H_6N_2O$, assay 98.5%, BDH, England

Nicotinic acid (NA), $C_6H_5NO_2$, assay 99%, Fluka, Switzerland

Nicotinaldehyde (NTA), $C_6H_5NO$, assay 98%, Aldrich, Germany

Tetraethyl orthosilicate (TEOS), $C_8H_{20}O_4Si$, assay 98%, Aldrich, U.S.A.

Ethanol (EtOH), $C_2H_6O$, commercial grade, Fluka, Switzerland

Methanol (MeOH), $CH_4O$, commercial grade, Fluka, Switzerland

Potassium cyanide, KCN, assay 97%, BDH, England

Pyridine, $C_5H_5N$, assay 99.5%, BDH, England

Acetonitrile (MeCN), $C_2H_3N$, analytical grade, RCI Labscan, Thailand

R.O. water, Department of Chemistry, Faculty of Science, Chiang Mai University, Thailand

### 2.2.2. Instruments

UV/Vis Spectrophotometer (Perkin Elmer, Lambda 25), U.S.A.

Scanning Electron Microscope (SEM) (JEOL, JSM 6335F), Japan

Transmission electron microscopy (TEM) (JEOL, JEM 2010), Japan

Fourier Transform Infrared (FTIR) Spectrometer (Bruker, TENSOR 27), Germany

Magnetight™ Separation Stand (Novagen), Germany

Incubator (Roche, COBAS EIA), Switzerland

Ultrasonic bath (Elma, S 30 H Elmasonic), 280 Watt, 50-60 Hz, Germany

### 2.2.3 Synthesis of magnetic nanoparticles (MNPs)

$Fe_3O_4$ nanoparticles were synthesized by chemical co-precipitation which reported by Molday [75]. Typically, a mixture of $FeCl_3$ (10.81 g, 0.04 mol) and $FeSO_4$ (5.56 g, 0.02 mol) was prepared under $N_2$ protecting, then, 20.0 ml of 30 % ammonia aqueous solution was dropped into it with violently stirring until the pH of the solution raised to 9. After 30 min, the resulting $Fe_3O_4$ nanoparticles were washed immediately with distilled water for several times and ethanol for 2 times by Magnetight™ separation stand. And then, $Fe_3O_4$ nanoparticles were dried into powder at 80 °C for 24 h. The morphology and size distribution of nanoparticles were examined by SEM and TEM.

### 2.2.4 Synthesis of aminopropyl magnetic silica

Aminopropyl magnetic silicas were prepared following previous reported procedure by Ma and co-workers [28]. Briefly, a certain amount of MNP powders were dispersed in a mixture of ethanol and water (100:1 v/v). The suspension was then subjected to ultrasonic for 30 min. Under rapid stirring, ATPES was added to the solution and was kept stirring at room temperature. After appropriate time, the suspended substance was separated by Magnetight™ separation stand, followed by washing several times with water and ethanol, then dried to powders at 80 °C for 24 hours. The loading of amino functional groups on surface of the aminopropyl modified MNPs were determine by quantitative ninhydrin method [76] (Table A.1).

### 2.2.5 Synthesis of magnetic molecularly imprinted silicas (M-MISs)

M-MISs were produced using NAM, NA and 3-APY as templates. APTES was used as monomer and tetraethyl orthosilicate (TEOS) was applied as cross-linking agent in basic aqueous media, in a molar ratio of 1:4:4 (template/monomer/cross-linker). Typically, a certain amount of aminopropyl magnetic silica was first dispersed in the mixture of EtOH: $H_2O$ (6:1 v/v). Then, 0.5 ml of ammonia solution and the silane precursor (APTES and TEOS) were added successively under vigorous stirring at room temperature. After 1 h, a stoichiometric amount of template molecule was added and was kept stirring for 24 h [33, 77]. The resulting M-MIS was separated from the mixture using Magnetight™ separation stand followed by washing with

copious water and ethanol. The template was then removed by washed with hot mixture of MeOH:$H_2O$ (4:1 v/v). Finally, the M-MIS products were dried at 80 °C for 24 h. An additional control batch (non-imprinted silica, M-NIS) was prepared following the above described procedure, in the absence of template.

### 2.2.6 Fourier transform infrared spectra (FT-IR) [78]

FT-IR was used to characterization of MNPs, aminopropyl magnetic silica, M-MISs and M-NIS. The samples for FT-IR analysis were prepared by grinding a quantity of the sample with dried potassium bromide (KBr) finely (to remove scattering effects from large crystals). This powder mixture is then pressed in a mechanical press to form a translucent pellet through which the beam of the spectrometer can pass. FT-IR spectra were recored on Fourier Transform Infrared (FTIR) Spectrometer (Bruker, TENSOR 27) at wavenumber 4000-500.

### 2.2.7 Transmission electron microscopy (TEM) [79]

TEM technique was used to examine particle size of the synthesized $Fe_3O_4$ MNPs. TEM specimen was prepared using a standard Holey carbon coated copper grids (grid sizes is a 3.05 mm diameter ring, 200 mesh). The sample dispersion was diluted with acetone and displaced a drop of diluted dispersion onto the inner meshed area of copper grid and let them dry before imaging. The size distribution particles

from enlarged photographs of the TEM images were measure using at least 100 counts of the particles.

### 2.2.8 Scanning electron microscopy (SEM) [79]

SEM was used to examine the morphology of all prepared materials including MNPs, aminopropyl magnetic silica, M-MISs and M-NIS. SEM specimens were prepared by diluting the particle dispersions with acetone and place one drop each on a copper tape which set up on a stub. The drop was allowed to dry at room temperature and then sputter coated gold prior to imaging.

### 2.2.9 Rebinding experiments

#### 2.2.9.1 Equilibrium batch rebinding studies

The binding efficiency and cross-selectivity test of M-MISs were determined by batch rebinding study using UV-Vis spectrophotometry. In general, a triplicate number of 10 mg quantities of both M-MIS and M-NIs were accurately weighed out in 1.5 ml microtube. To each magnetic silica was added 1.0 ml of a 0.2 mM binding species in the selected media. After incubating at room temperature, the M-MIS was separated by Magnetight™ separation stand. Then, the UV absorbance of the clear supernatant was measured with a Lambda 25 UV/Vis spectrophotometer with 1 cm quartz cells. The maximum wavelengths for each template molecule are at λ 262 nm

for NA and NAM and at λ 238 nm for 3-APY. This experiment was performed in triplicate for each M-MIS. Percentage bound (%Bound) of the analyte was calculated according to this equation;

$$\%\text{Bound} = (Q/Q_{initial}) \times 100$$

When Q is the amount of analyte bound to polymer, was calculated by subtracting the concentration of free analyte from the initial analyte loading, $Q_{initial}$ is the amount of analyte unbound to polymer. This experiment was done in triplicate for each polymer.

The imprinting factor (α) used as a measurement of the strength of interaction between the template and MIPs were calculated according to the following equation;

$$\alpha = \frac{\text{M-MIS}_{(bound)}}{\text{M-NIS}_{(bound)}}$$

Where $\text{M-MIS}_{(bound)}$ is the %Bound of the M-MIS, while $\text{M-NIS}_{(bound)}$ is the %Bound of the M-NIS.

The selectivity factors were calculated according to the following equation:

$$\acute{\alpha} = \frac{B_{analogue}}{B_{template}}$$

Where $B_{analogue}$ is the %Bound of the M-MISs with NA, while $B_{template}$ is the %Bound of the M-MISs with corresponding template.

### 2.2.9.2 Adsorption kinetic of NA onto M-MIS 1

To investigate the adsorption kinetics of NA onto M-MIS **1**, 30 mg M-MIS **1** was dispersed in methanol solution of 0.2 mmol/L NA (10 ml). The mixture was incubated continuously at room temperature. The specimens were sampled at different time intervals: 15, 30, 60, 120, 180 and 300 min. The binding efficiency was determine using UV-Vis spectrophotometry as same as previously described procedure.

### 2.2.9.3 Scatchard analysis

10.0 mg of M-MIS **1** was equilibrated with varied initial concentration (0.1, 0.2, 0.3, 0.4, 0.5, 1.0 and 1.5 mM) of NA in methanol. After 1 h, the saturated M-MIS **1** was separated by a Magnetight™ separation stand. The supernatant was analyzed by UV-Vis spectrophotometer. All experiments were done in triplicate.

### 2.2.9.4 Binding selectivity of M-MIS 1

In order to estimate the selectivity of M-MIS **1**, the selectivity test of M-MIS **1** and its corresponding M-NIS were carried out using a series of NA structurally related compounds including NA, BZA, C-NA, NTA, NAM and 3-APY. The amounts of bound to the M-MISs were determined by batch rebinding. To the solution of tested compounds (0.2 mM in EtOH) were added with the M-MIS **1** (10 mg). The sample was incubated on the shaking incubator for 1 h at room temperature. Then, the M-MIS **1** was separated by Magnetight™ separation stand and the supernatant was analyzed by UV-Vis spectrophotometer at the maximum wavelength of each compound. The amount of bound to M-MIS **1** was revealed from %Bound which performed using the previously described procedure. This experiment was performed in triplicate for each test compound.

### 2.2.9.5 Regeneration of M-MIS 1 and its reusability

The M-MIS **1** with adsorbed species was regenerated by sonication 5 minute for 5 times in methanol or until the final filtrate showed no trace of binding analytes as determined by TLC. The solid M-MIS **1** was separated by a Magnetight™ separation stand and rinse with acetone, dried in oven at 60 °C, and reused for the subsequent adsorption of NA.

## 2.3 Results and Discussion

### 2.3.1 Synthesis and characterization of MNPs

Magnetic nanoparticles of $Fe_3O_4$ were synthesized by chemical co-precipitation of $Fe^{3+}$ and $Fe^{2+}$ salts in aqueous media. The synthesis of particles was done in an oxygen-free environment by passing $N_2$ gas into the reaction mixture. After adjust the pH to 9 with aqueous ammonia solution, the black precipitate of magnetite nanoparticles, MNPs, were formed. As shown in Fig. 2.3, the prepared MNPs are susceptible to magnetic fields and could easily and quickly be separated from a suspension.

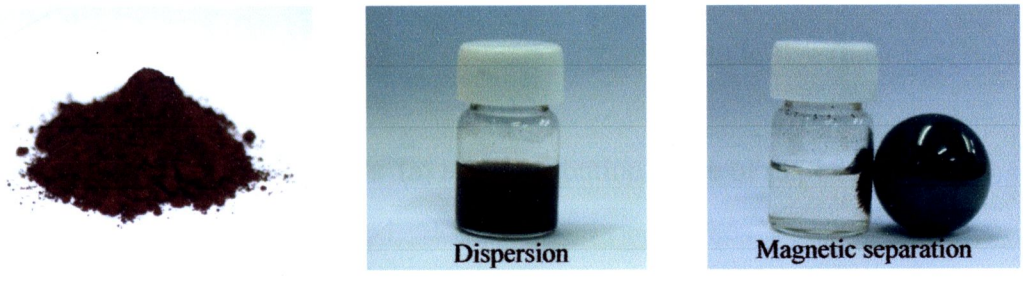


**Figure 2.3** The physical appearance and magnetism properties of MNPs

The size and shape of the $Fe_3O_4$ MNPs were examined by TEM analysis. TEM image (Fig. 2.4) revealed that the MNPs appear almost spherical and tend to form aggregations, indicating a ferromagnetic interaction [80]. The distribution curve of the particles size showed the diameter of MNPs in the range of 9–26 nm with an average diameter of 20 nm. The particle size of the synthesized MNPs was slightly greater

than these of previous report on $Fe_3O_4$ nanoparticles (6–15 nm) [81]. These differences may be due to the effect of synthesis conditions depending on type of salts used (e.g. chlorides, sulphates, nitrates, perchlorates, etc.), $Fe^{2+}$ and $Fe^{3+}$ ratio, pH and ionic strength of the media [81].

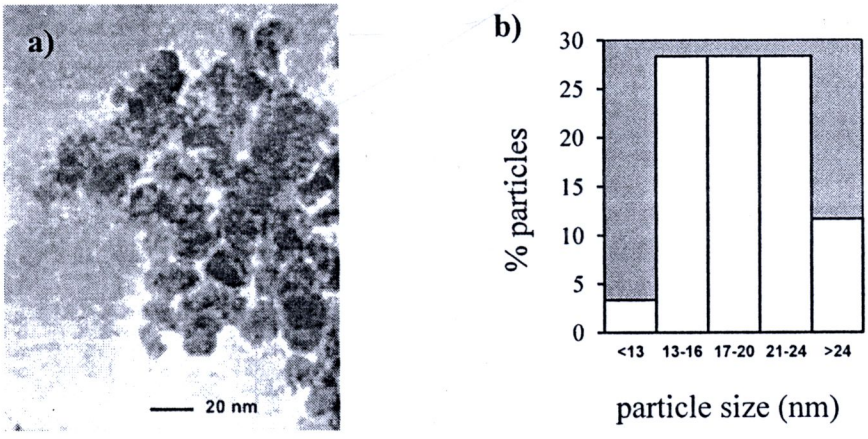


**Figure. 2.4** TEM image of MNPs (a) and distribution curve of particle size (b)

### 2.3.2 Surface modification and characterization of modified MNPs

Chemical modifications of inorganic materials using alkoxysilanes have been reported [28, 82, 83]. As shown in Fig. 2.5, the surface hydroxyl groups of $Fe_3O_4$ nanoparticles were reacted with the ethoxy groups of APTES to form aminopropyl functionalized MNPs.

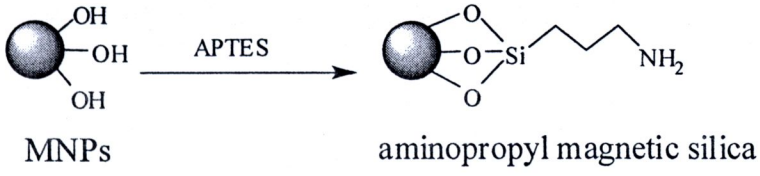


**Figure. 2.5** Synthesis of aminopropyl magnetic silica

The loading of aminopropyl group on the surface of MNPs was studied by varying percentage of APTES volume/ MNPs weight ratio and reaction times. The effect of the amount of APTES was studied using 100 mg of MNPs and APTES at 10, 20, 30, 40 and 50% v/w.

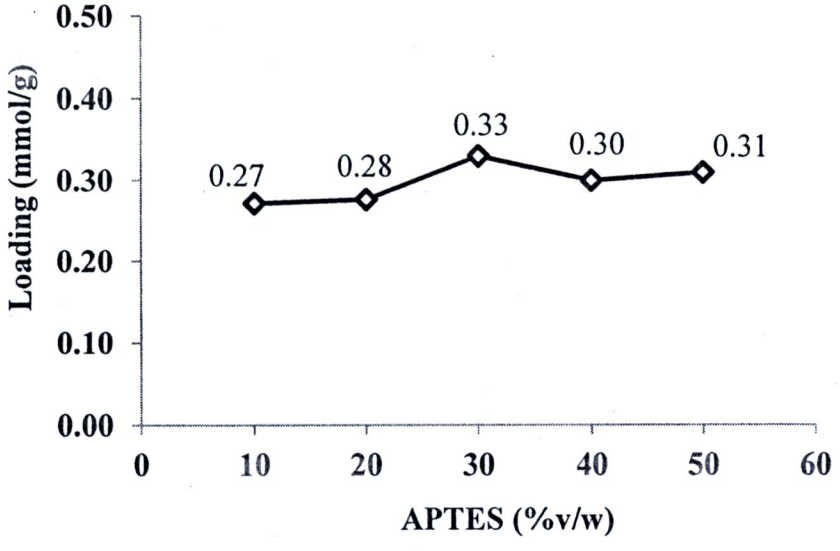


**Figure. 2.6** The effect of APTES volume/ MNPs weight ratio to loading of amino group on aminopropyl magnetic silica surface after 7 h reaction time

Fig. 2.6 shows that loading capacity of aminopropyl group on the magnetic silica increases slightly with increasing the percentage of APTES from 10 to 30%. However, the loading become steady with further increase in APTES amount. The maximum loading of the aminopropyl group at 0.33 mmol/g was obtained when using 30 %v/w of APTES.

To determine the appropriate reaction time, the reaction of MNPs and APTES was carried out by treating 100 mg of MNPs with 30 μL APTES (30% APTES v/w) at room temperature for 0.5, 1, 2, 3, 5, 7 and 9 h. The aminopropyl loading of aminopropyl magnetic siliscas at different time (in hours) intervals were shown in Fig. 2.7. The highest aminopropyl loading of 0.33 mmol/g was achieved at 5 h reaction time. The amino loading was almost unaffected at longer reaction time. It may be due to the decrease in the availability of the reactive hydroxy group on $Fe_3O_4$ surface, both in number and in accessibility. Therefore, 5 h is a required time for maximum loading of the aminopropyl group.

The optimal conditions (30% v/wt of APTES/MNPs, 5 h at room temperature) will be used for scale up reaction in order to prepare the aminopropyl magnetic silica for use in further experiments.

It is noted that the aminopropyl modified magnetic silica do not show any difference in physical appearance and magnetism property comparing to the unmodified MNPs (data not shown). This result is in accordance with previous report [28, 29, 82]. It may be suggested that modification method has no effect on the magnetism property of the modified MNPs.

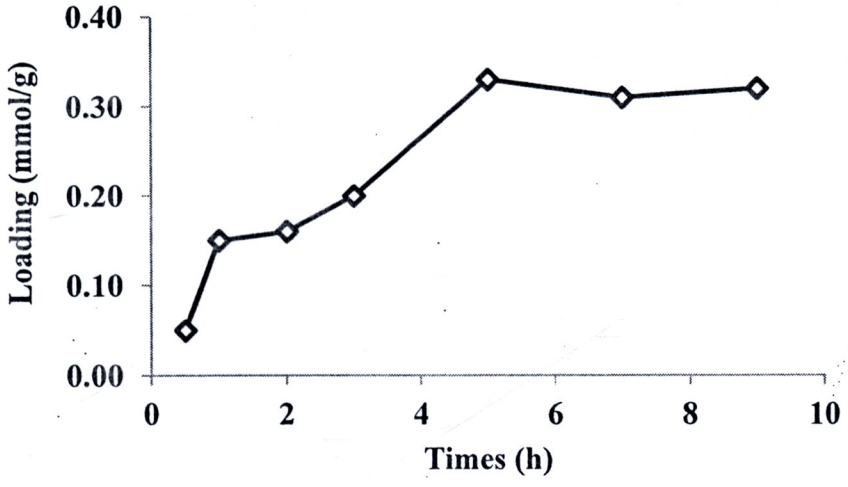


**Figure. 2.7** The effect of reaction times to loading of amino group on aminopropyl magnetic silica surface

### 2.3.3 Synthesis and characterization of M-MISs

Three M-MISs were synthesized with three different template molecules. NA , a target compound, is a representative of an acidic functionalized molecule, while NAM and 3-APY represent a neutral and a basic functionalized molecule, respectively. All of these M-MIS types were synthesized using sol-gel technique. After incubation of aminopropyl magnetic silica and silane precursor with template molecules, follow by hydrolysis and polycondensation, the three-dimensional polysilicate network of M-MIS **1-3** can be obtained (Fig. 2.8). The structure of templates, silane monomer and cross-linker used for synthesis M-MISs are shown in Fig. 2.9.

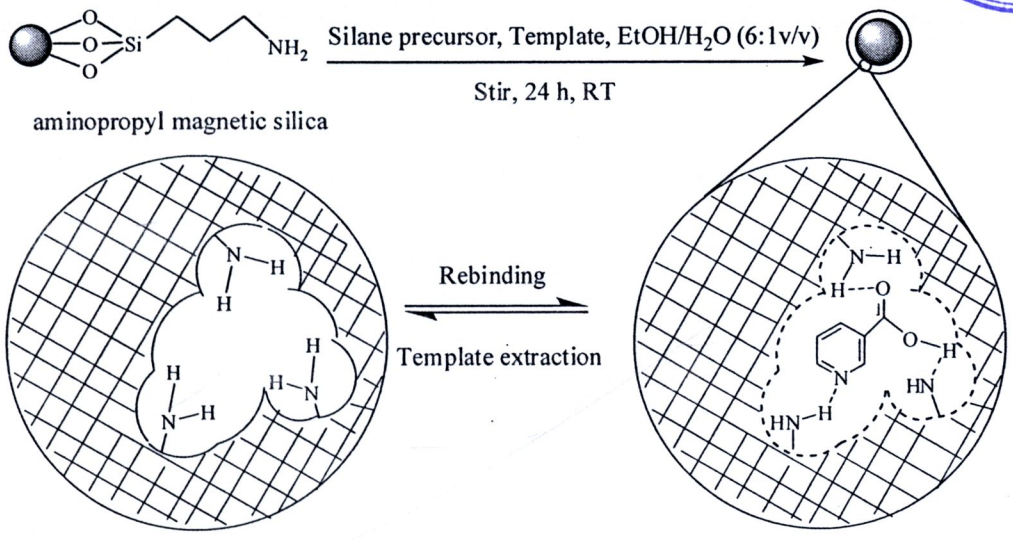


**Figure. 2.8** Schematic illustration for synthesis of M-MIS with NA template

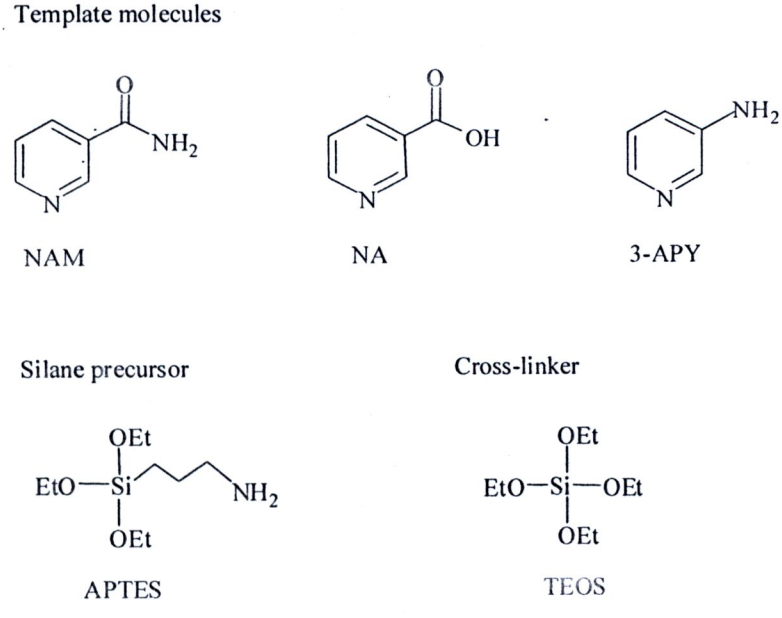


**Figure. 2.9** Structure of templates, silane precursor and cross-linker used in M-MIS synthesis

The compositions, yields and physical appearance of the obtained M-MISs were also shown in Table 2.2. The modification of aminopropyl magnetic silica with silane precursors similarly produced M-MIS **1**, **2** and **3** as brown powder with comparative yield.

**Table 2.2** Compositions, yield and physical appearance of the synthesized M-MISs and M-NIS

| **Modified MNPs** | **Template** | **APTES/TEOS/ Template** | **% Yield** | **Physical appearance** |
|---|---|---|---|---|
| M-MIS **1** | NA | 4:4:1 | 45 % | Brown powder |
| M-MIS **2** | NAM | 4:4:1 | 44 % | Brown powder |
| M-MIS **3** | 3-APY | 4:4:1 | 45 % | Brown powder |
| M-NIS | - | 4:4:0 | 60 % | Brown powder |

FT-IR spectroscopy was used to study the chemical structure of the imprinted-, and the non-imprinted magnetic silicas in comparison with MNPs and aminopropyl magnetic silica. As shown in Fig. 2.10. A sharp and strong Fe-O stretching peak (~586 $cm^{-1}$) was observed for bulk MNPs and in all of the surface modified samples, indicating that the main structure was not changed by the modification [66, 84]. The absorption bands at ~2865 $cm^{-1}$ and 2938 $cm^{-1}$ (C-H stretching), 1500-1600 $cm^{-1}$ (N-H bending), 1075 $cm^{-1}$ (Si-O stretching) of aminopropyl magnetic silica, M-MISs and M-NIS indicated the presence of aminopropyl groups [66]. All of these results reveal the existence of APTES component in all samples. Meanwhile, in Fig 2.10c-f of M-MISs and N-MIS, the existence of TEOS could be confirmed by the appearance of a very sharp and strong adsorption bands of SiO-H and Si-O-Si of silica matrix at 1060 $cm^{-1}$ [66]. The above results confirmed that MISs were coated onto the MNPs. Moreover, The most distinctive absorption band found in all samples at 3450 $cm^{-1}$ and 1630 $cm^{-1}$ are corresponded to the stretching of O-H and N-H bonds, and it is attributed to non-condensed silanols, residual water and also to the aminopropyl groups linked to the silica network [28]. For M-MIS and M-NIS, there is no substantial difference in the IR absorption bands; any possible difference between these materials, specially their sorptive properties, should presumably be due to the morphological differences caused by the molecular imprinting process.

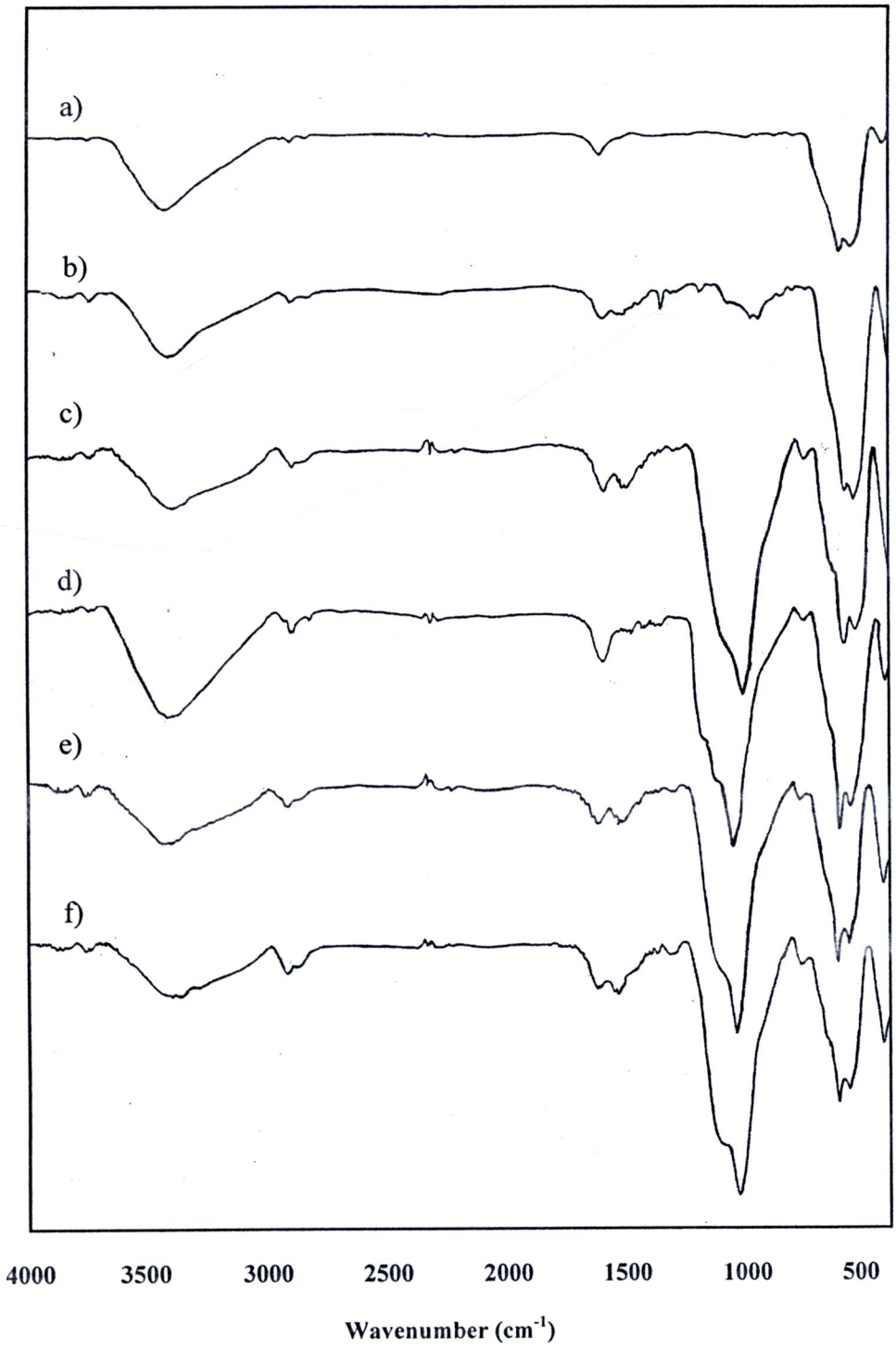


**Figure. 2.10** FT-IR spectrum of (a) MNPs, (b) aminopropyl magnetic silica (c) M-MIS **1**, (d) M-MIS **2**, (e) M-MIS **3** and (f) M-NIS

The morphology of all synthesized materials comprising of MNPs, aminopropyl magnetic silica, M-MISs and their corresponding M-NIS were studied with SEM technique. According to Fig. 2.11, all of synthesized materials are agglomerate of spherical beads which could be due to effect of ferromagnetic interaction [80]. Apart from the particle size, no significant differences in the appearance of all samples were observed.

### 2.3.4 Rebinding experiments

#### 2.3.4.1 Binding characteristics of M-MISs in 6:1 (v/v) EtOH/$H_2O$ mixture

The rebinding experiment is used to evidence the imprinting effect of M-MIS by comparing the rebinding efficiency of M-MIS to the corresponding M-NIS. Rebinding efficiency of the M-MISs were evaluated from the quantity of template bound to M-MIS which were calculated in term of %Bound.

The imprinting effect of M-MIS related to non-imprinted one can be evaluated from the imprinting factor ($\alpha$). The imprinting effect is evidenced when the $\alpha$ value is >1.

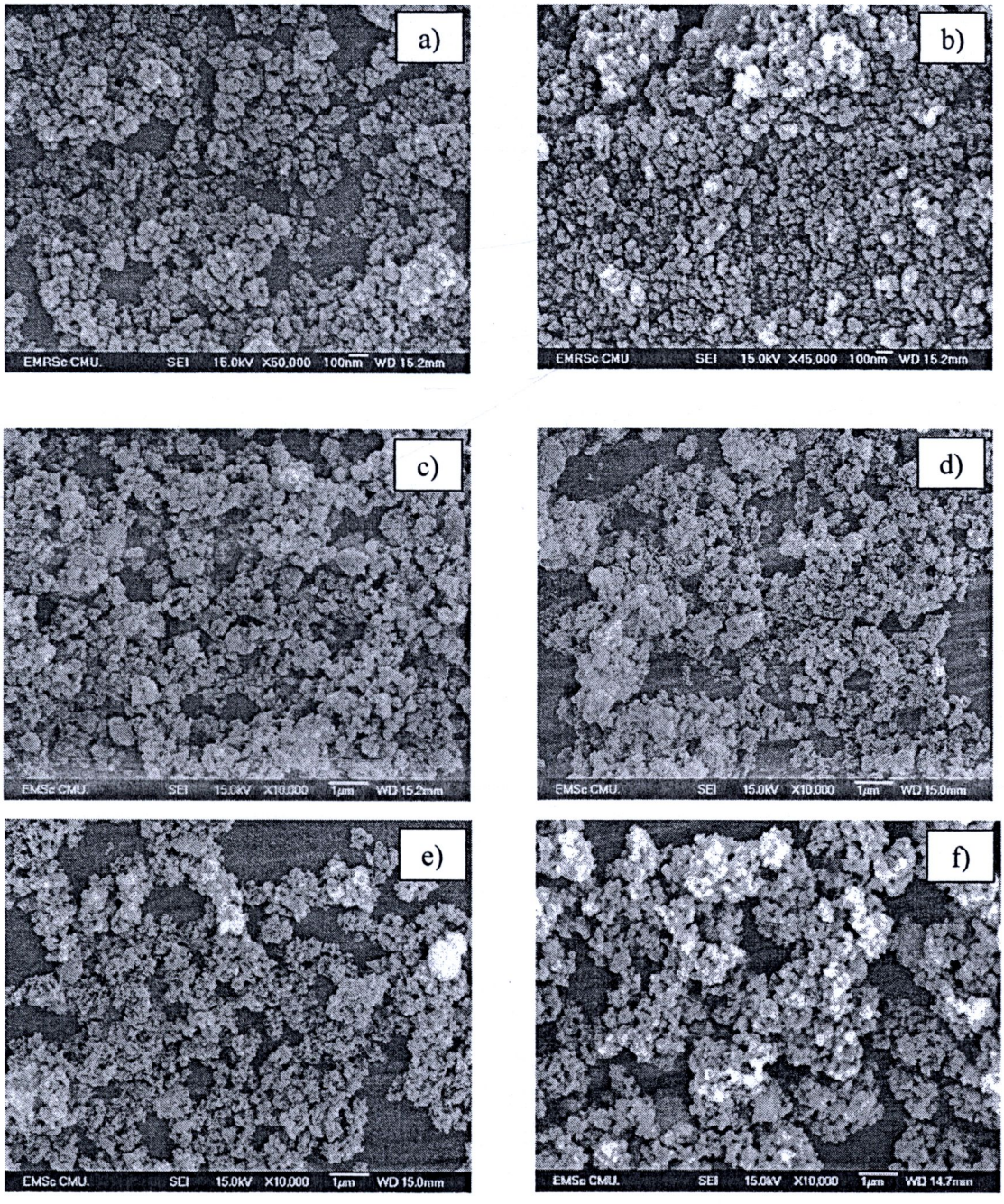


**Figure. 2.11** SEM image of (a) MNPs (50,000X), (b) aminopropyl magnetic silica (45,000X), (c) M-MIS **1** (10,000X), (d) M-MIS **2** (10,000X), (e) M-MIS **3** (10,000X) and (f) M-NIS (10,000X)

In preliminary study, the recognition abilities of all MISs toward their corresponding templates were investigated in a mixture of 6:1 (v/v) EtOH/$H_2O$ which is a media used in the imprinting process. The %Bound of MISs and the imprinting factors of MIPs were shown in Table 2.3. Among all the tested M-MISs, M-MIS **1** showed the highest percentage bound of NA with the highest imprinting factor (2.04). It is noted that the negative %Bound of 3-APY observed in case of M-MIS **3** may be due to the interference of the template bleeding that can be observed when template is not completely removed in the template extraction step.

**Table 2.3** Binding characteristics of M-MISs in 6:1 (v/v) EtOH/$H_2O$ mixture after 1 h incubation

| M-MIS | Template | %Bound$_{template}$ | α | %Bound$_{NA}$ | ά |
|---|---|---|---|---|---|
| M-MIS **1** | NA | 32.05 | 2.04 | 32.05 | 1.00 |
| M-MIS **2** | NAM | 13.48 | 1.25 | -1.50 | nd |
| M-MIS **3** | 3-APY | -4.63 | nd | 13.26 | 0.41 |

It has been postulated that each of template-monomer complex in the pre-polymer solution gives rise to each binding site. Increasing the degree of complementary order or binding affinity of the complex in the prepolymerization mixture would increase the number of final binding sites in the imprinted silica. The

NA templates used in the aforementioned studies is a pyridine ring attaching with carboxylic functional group whereas NAM and 3-APY are pyridine ring functionalized with amide and amino group, respectively. An acidic residue on NA provides strong ionic interaction with the basic side chain of APTES monomer leading to high order of template-monomer complex formation and give rise to the forming of recognition cavity in silica matrix. Hence, the higher %Bound and imprinting factor were evident. Whereas NAM and 3-APY which have a neutral and basic functional group, respectively, could only form a few weak, non-covalent bonds with aminopropyl side chains of APTES resulting in weak template-monomer complex formation as confirmed by the observed low percentage bound of their templates with low imprinting factor.

When considering aqueous solubility of all template molecules, NA is less soluble in water than NAM and 3-APY suggested NA is the most hydrophobic followed by NAM and 3-APY, respectively. Therefore, binding of the more hydrophobic molecules to their corresponding M-MIS in aqueous media can be facilitated by hydrophobic interaction causing higher percent bound observed in M-MIS **1**. On the contrary, NAM and 3-APY are more soluble in aqueous media, these compound thus has less potential to bind to M-MIS.

Effect of acidic NA substrate on binding performance of the MISs was studied. As shown in Table 2.3, M-MIS **1** showed a highest binding efficiency with NA with the highest selectivity factor in comparative to M-MIS **2** and M-MIS **3**. These results

indicated that binding of NA to M-MIS **1** is strongly due to selectively recognition and not merely the results from hydrophobic nonspecific binding.

From the results, it can be concluded that M-MIS **1** exhibited the best binding performance to NA as indicated from its high percent bound of NA and imprinting factor. The interactions between the template molecule and specific cavities of M-MIS **1** are presumably predominated by electrostatic ionic interactions.

### 2.3.4.2 The effect of binding media to the binding efficiency of NA to M-MIS 1

In general, molecular imprinted materials perform better in the solvent used in their syntheses because this solvent is able to recreate the interactions that took place during the pre-polymerization [64, 85, 86]. However, effective recognition of imprinted materials can be obtained in media other than that used as synthetic solvents, including aqueous buffers [43, 87]. In this case a switch in recognition mechanism from H-bonding to hydrophobic recognition can be demonstrated by a loss of recognition in intermediate aqueous–organic mixtures [88].

To determine the suitable media for NA rebinding, the binding efficiency for M-MIS **1** and M-NIS **1** in the various media was studied. The results of percent bound of NA to M-MIS **1** and M-NIS were shown in Fig. 2.12. Type of media has a significant effect on binding efficiency of M-MIS **1** toward NA. In pure MeCN (dielectric constant, $\varepsilon$ = 37.5 [89]), NA can be bound to M-MIS **1** with the highest %Bound (91.7±2.6%) but the binding was highly nonspecific ($\alpha$ ~1). When pure

EtOH ($\varepsilon$ = 25.1 [89]) and MeOH ($\varepsilon$ = 33.6 [89]) were used as the media, the binding efficiency of NA on to M-MIS1 in EtOH is slightly superior to that one in MeOH. These results suggested that polar protic solvent can interfere with the interactions taking place in the binding cavities.

The binding efficiency of M-MIS **1** in EtOH decreases with increasing the water content. A similar trend was observed in MeCN and MeCN/$H_2O$ systems (>90 %Bound as opposed to < 20 %Bound). The decrease in the percentage bound of NA to the imprinted sol-gel could be resulted from the salvation power of water. Water is a highly polar protic solvent ($\varepsilon$ = 80.4 [89]) which can solvate NA molecule and the binding cavities of M-MIS. Solvation of $H_2O$ molecules can strongly disturb in the interaction between NA and M-MIS leading to the decrease of %Bound of NA onto M-MIS **1**.

The specific binding of M-MIS **1** in each medium can be evidenced by imprinting factor value. According to Fig. 2.12 (b), the greatest specificity ($\alpha$ = 4.35) was observed in 4:1(v/v) MeCN/$H_2O$ mixture. Despite this condition provide specific binding but %Bound of NA in this mixture is lowest compared to other media. Some degree of discrimination between M-MIS and M-NIS still exists in EtOH. On the basis of these results, EtOH will be used as the media in subsequent experiments to further study binding characteristics of M-MIS **1**. It is noted that in previous report, NA binds to the imprinted polymer with imprinting factor in a range of 1.27-3.05 [90]. This data suggest the types of polymer matrices can play an important role in molecular recognition.

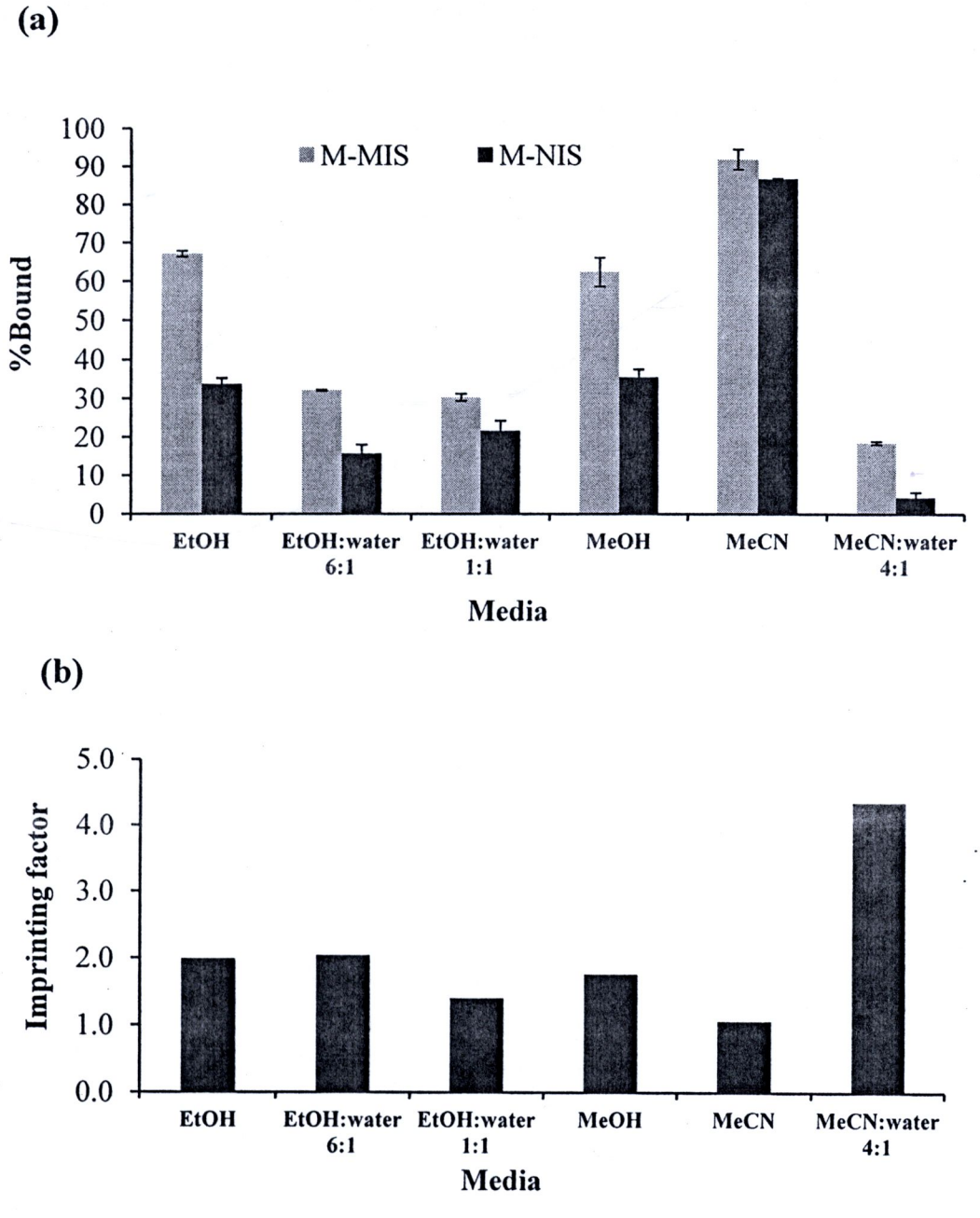


**Figure 2.12** %Bound (a) and imprinting factor (b) of NA onto M-MIS **1** in various media

### 2.3.5 Adsorption kinetic of NA onto M-MIS 1

The rate of NA rebinding was further studied since it is one of the important considerations for the practical application of the M-MIS. The experiments were performed by estimation of binding efficiency by changing the adsorption time from 0 to 300 min and the initial concentration of NA was kept constantly at 0.2 mmol/L. An adsorption kinetic curve was presented in Fig. 2.13.

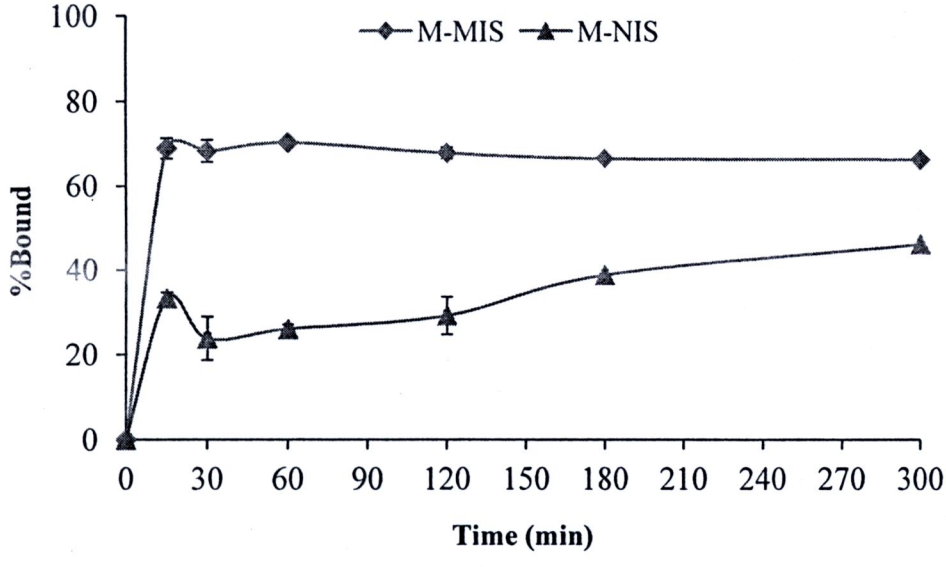


**Figure 2.13** Adsorption kinetic curve for binding of NA on to M-MIS **1**

The typical kinetic curve for most rebinding processes was observed revealing the M-MIS **1** reached the maximum adsorption within 15 min. Considering that the sol-gel imprinted particles reported previously often required more than one hour for achieving the highest adsorption ability [63, 64, 66, 68]. This surprisingly fast

kinetics may result from the surface imprinting approach [33, 91-93] and it is consistent with the high porous silica network with recognition cavities created over the magnetic particle surface. Therefore, most of imprinted cavities are situated at the surface of M-MIS which makes the recognition sites accessible for the template molecules and thus take shorter time to gain adsorption equilibrium.

In case of M-NIS, similar rate of NA rebinding was observed. However, equilibrium was not reached up to 300 min. It is presumed that NA only bound to M-NIS with weak physical interaction due to the lack of specific binding cavities in silica matrices of M-NIS.

### 2.3.6 The binding isotherm

According to the concept of molecularly imprinting strategy, it is expected to develop materials which provide high affinity to target molecule. In characterizing the adsorption behaviors of the M-MIS and M-NIS particles, they were subjected to rebinding equilibrium and kinetics studies. Batch rebinding tests were performed at different initial concentration of NA, ranging from 0.1 to 1.5 mmol/L. Fig. 2.14 and Fig. 2.15 show the %Bound NA and binding capacity of M-MIS **1** at different equilibrium concentration. Within the concentration range studied, the M-MIS particles exhibited much higher binding capacity than the controlled M-NIS particles.

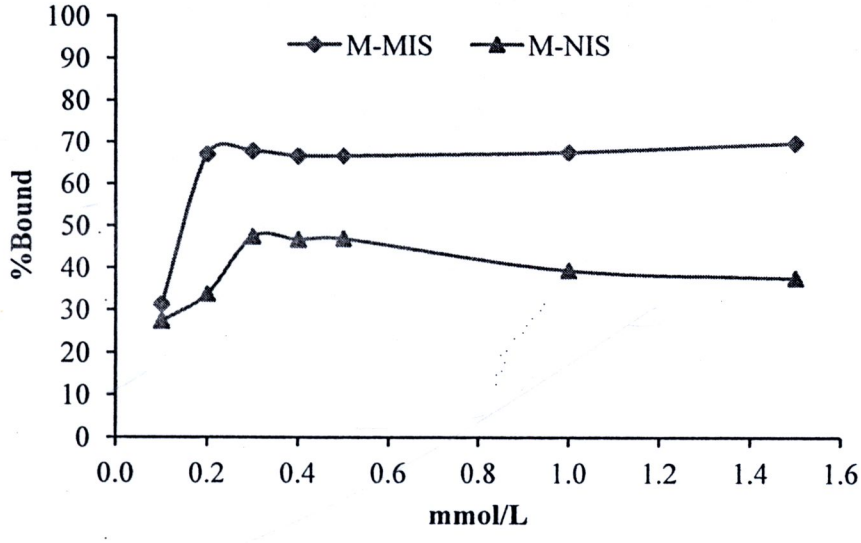


**Figure 2.14** %Bound of M-MIS **1** in various NA concentration

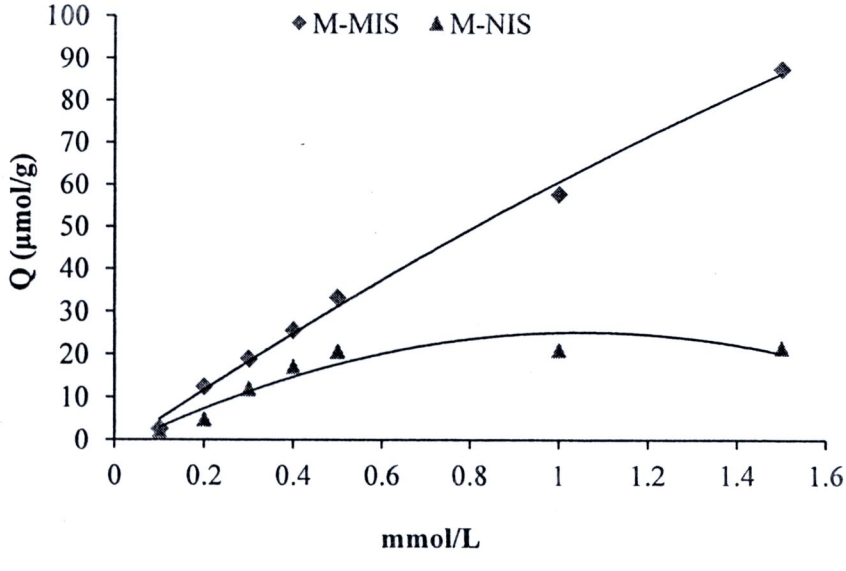


**Figure 2.15** Adsorption isotherm of NA onto M-MIS **1**

It is very difficult to obtain information about the imprinted (and other, non-imprinted) binding sites of the molecularly imprinted materials by direct, e.g. spectroscopic methods. For this reason, most of our knowledge about the concentration and binding strength (affinity, binding constant) of the sites has been derived from mathematical analysis of adsorption isotherms. Such analyses are essentially based on the assumption of a binding model, e.g. Langmuir, bi-Langmuir, Freundlich or other, and obtaining the parameters of the model from curve fitting to the measured isotherm [94].

After the linear model based on a linear dependence between the adsorption rate and the number of free binding sites, the simplest and more frequently used model in adsorption studies is the Langmuir one. This isotherm is based on three assumptions [95]: (a) adsorption cannot proceed beyond monolayer coverage, (b) all surface binding sites are equivalent and can accommodate, at most, one adsorbed template and (c) the ability of a template to bind at a given site does not depend on the occupation of neighbouring sites.

A basic assumption of the Langmuir theory is that sorption takes place at specific homogeneous sites within the adsorbent. It is then assumed that once a template molecule occupies a site, no further adsorption can take place at that site. Therefore, a saturation value is reached beyond which no further sorption can take place [95-97]. This value allows the calculation of the surface binding capacity. The Langmuir equation is represented as follows [92]:

$$Q_e = Q_m \cdot C_{eq} / (K_d + C_{eq})$$

where $C_{eq}$ (μmol/ml) is the equilibrium concentration of NA in bulk solution, $Q_{eq}$ (μmol/g) is the amount of adsorbed NA on per gram of the M-MIS particles at the equilibrium concentration, $Q_m$ (μmol/g) is the maximum capacity and $K_d$ (μmol/ml) is the affinity constant of the adsorbent.

The Langmuir isotherm equation can be transformed into linear forms to obtain adjustable parameters just by graphical means or by a linear regression analysis. Rewriting equation as :

$$\frac{1}{Q_{eq}} = \frac{1}{Q_m} + \frac{1}{K_d Q_m C_{eq}}$$

The constants $Q_m$ and $K_d$ can be determined by plotting $1/Q_{eq}$ versus $1/C_{eq}$.

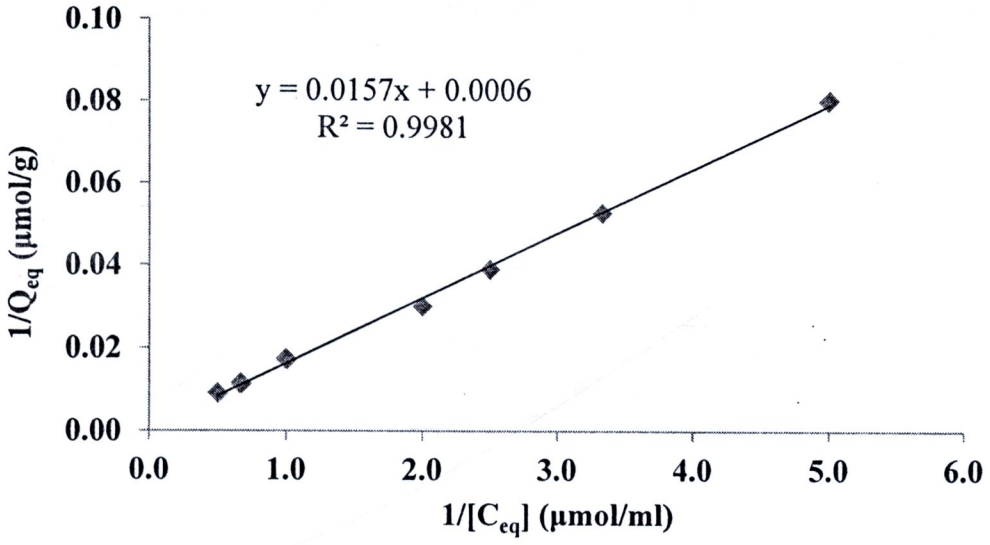


**Figure. 2.16** Langmuir plot of the adsorption of NA on to M-MIS **1**

By fitting the experimental data with Langmuir equation, it can be implied that the rebinding of NA to M-MIS **1** is monolayer adsorption. Fig. 2.16 represented Langmuir plot of the adsorption of NA on to M-MIS **1**. The estimated $Q_m$ and $K_d$ are 1,666.67 µmol/g and 0.0382 µmol/ml for the M-MIS particles, and 13.79 µmol/g and 1.3577 µmol/ml for the M-NIS particles, respectively. The lower $K_d$ for the M-MIS particles corresponds to their higher affinity toward NA molecules. The fact that the experimental data agreed well with the Langmuir isotherm implies a homogeneous distribution of molecularly imprinting adsorption sites on the M-MIS surface.

The saturation binding data were further processed with Scatchard equation to estimate the binding affinity of imprinted magnetic nanoparticles. The Scatchard

equation derived on the basis of a uniform site-binding model (binding of ligands to independent indistinguishable sites on the polymer) was as follows [74]:

$$Q_{eq}C_f = Q_mK_d - Q_{eq}K_d$$

where $Q_{eq}$ (μmol/g) is the amount of NA bound to M-MIS at equilibrium, $Q_m$ (μmol/g) is the apparent maximum number of binding sites, $C_f$ (μmol/ml) is the free analytical concentration at equilibrium and $K_d$ (μmol/ml) is the affinity constant. Likely to Langmuir equation, the Scatchard equation can be transformed into linear forms to obtain adjustable parameters just by graphical means or by a linear regression analysis. The linear equation of Scatchard plot is expressed as :

$$Q_{eq}/C_f = K_dQ_m - K_dQ_{eq}$$

The values of $K_d$ and the $Q_m$ can be calculated from the slope and intercept of the linear line plotted in $Q_{eq}/C_f$ versus $Q_{eq}$.

Scatchard analysis was performed in the present study. According to the Scatchard plot of M-MIS 1 in Fig. 2.17, the plot was a single straight line, which indicated the binding sites of M-MIS particles were identical. The sol-gel technique combines the advantages of non-covalent imprinting strategy provided the M-MIS to assemble sites that bind the target molecules in a non-covalent fashion. The linear regression equation for the linear region is $Q/C_f = 179.9-0.5208Q_{eq}$. From the slope

and the intercept of the straight line obtained, the values of $K_d$ and $Q_m$ were 0.5208 μmol/mL and 345.43 μmol/g, respectively.

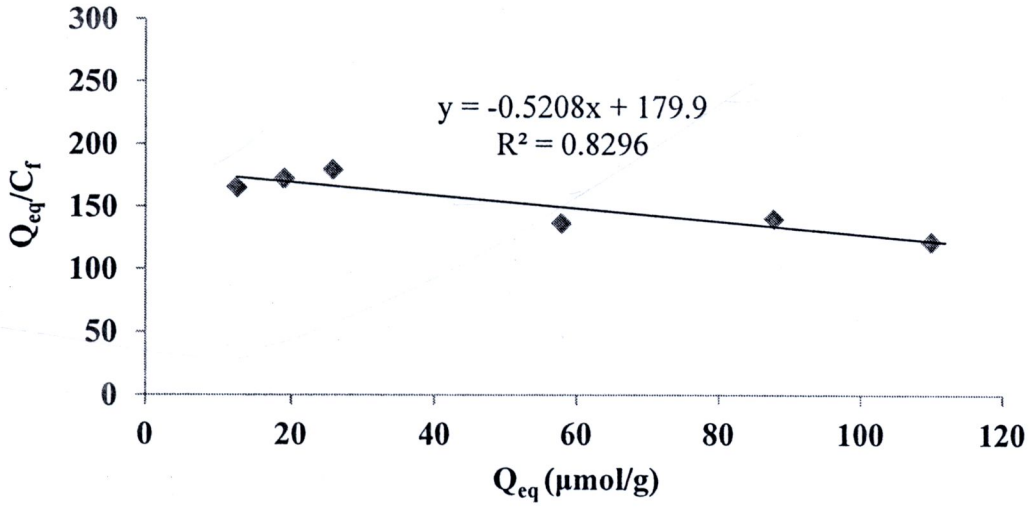


**Figure 2.17** Scatchard plot of M-MIS **1** for NA

To compare the reliability of these models of interaction, the $Q_m$ and $K_d$ for each model of interaction was summarized in Table 2.4. Based on the values of the interaction constant ($K_d$) for the two plots, the Scatchard plot gives information regarding the complex formation whereas the Langmuir adsorption isotherm gives the cule involving the physical adsorption.

As shown in Table 2.4, $Q_m$ from Langmuir adsorption model is larger than that from Scatchard model. This result can be reasoned that the binding behavior of NA molecules onto M-MIS is predominant physical adsorption. Moreover, it can be also

confirmed by $K_d$ value, the lower $K_d$ for the M-MIS from Langmuir analysis indicated more effective physical adsorption than the complex formation.

**Table 2.4** The binding constant and the maximum number of binding sites of M-MIS

| **Adsorption model** | **$K_d$ (μmol/mL)** | **$Q_m$ (μmol/g)** |
|---|---|---|
| Langmuir model | 0.0382 | 1,666.67 |
| Scatchard model | 0.5208 | 345.43 |

### 2.3.7 Selectivity evaluation

The selectivity of the M-MIS **1** was investigated using BZA, C-NA, NTA, NAM and 3-APY as the structural analogues of NA template. Their chemical structures are shown in Fig.2.18. The experiment was carried out in ethanol as previously described in the batch rebinding experiments.

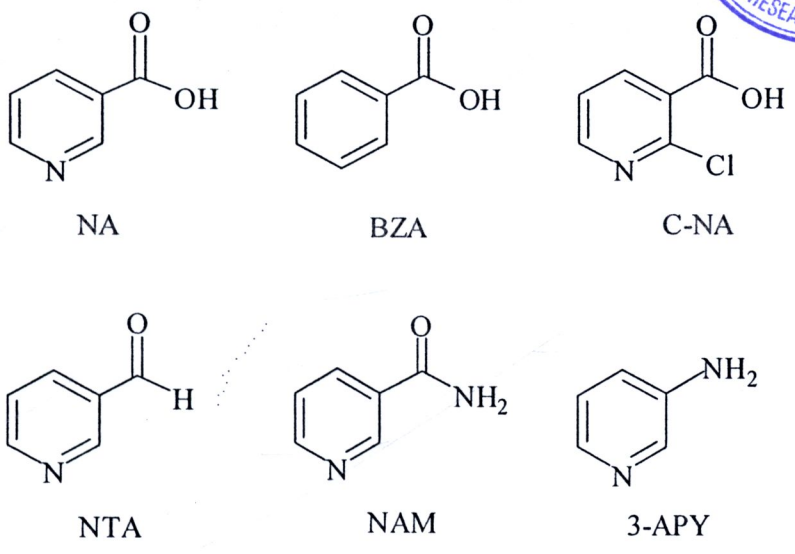


**Figure 2.18** Structure of compounds used in selectivity study

Fig. 2.19 (a) shows the %Bound of NA, BZA, C-NA, NTA, NAM and 3-APY with the M-MIS **1** and M-NIS. In most case, the %Bound of NA and its analogues on the magnetic MIS were higher than those on the magnetic NIS. There was no obvious difference in the adsorp amount of NAM and 3-APY on both M-MIS and M-NIS.

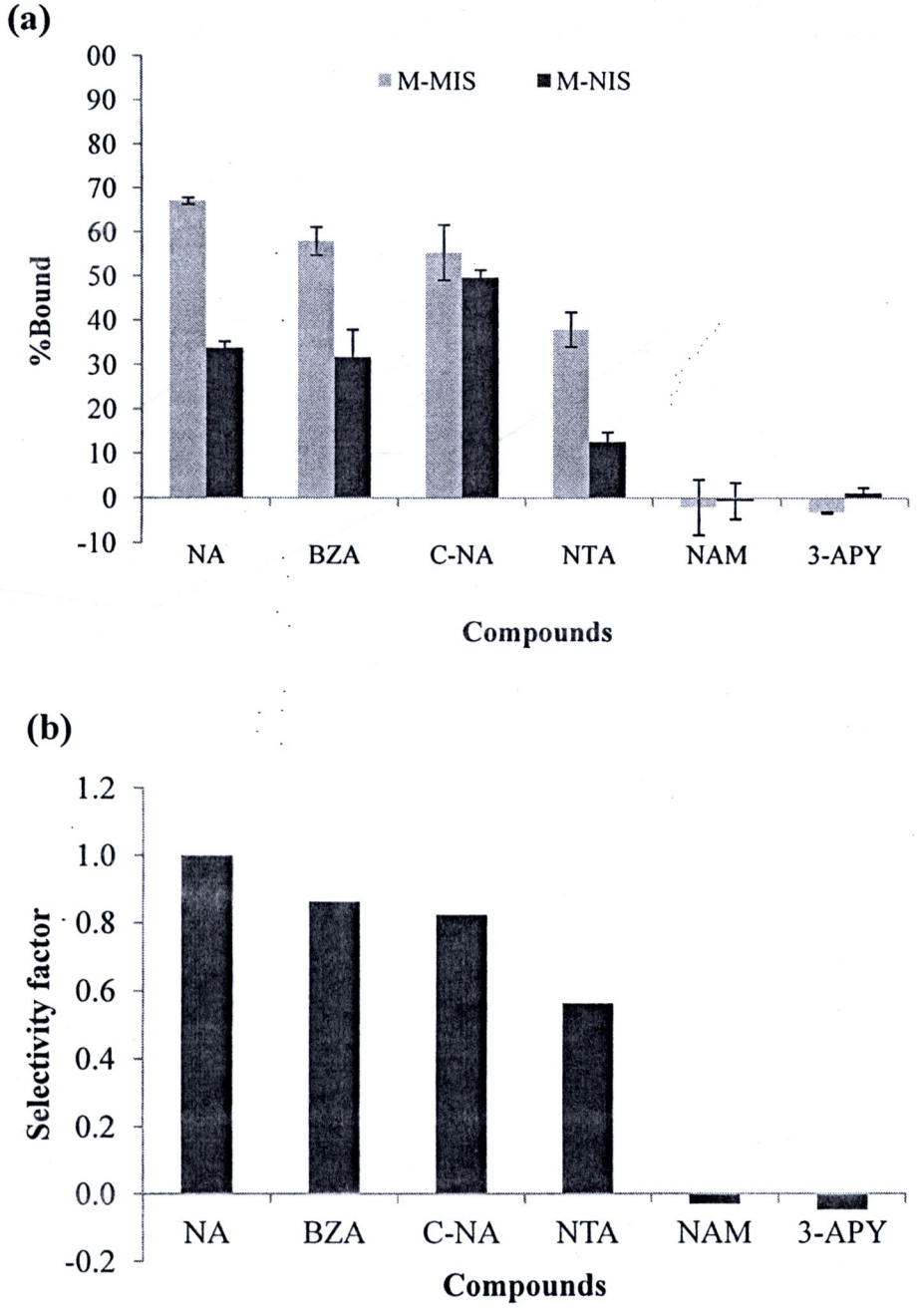


**Figure 2.19** %Bound (a) and selectivity factor (b) of NA and its analogues on to M-MIS **1**

Considering, the selectivity factor of NA and its analogues as shown in Fig. 2.19 (b), M-MIS **1** exhibited higher selectivity to NA than other tested substrates. The results clearly confirmed the effectiveness of the molecular imprinting process where the NA imprinted magnetic silica provided efficiently selective binding to its template NA. The high selectivity is mainly due to complementary in both shape and functionality of silica matrix to NA template.

### 2.3.6.7 Study of M-MIS reusability

Owing to the advantages of the participation of a magnetic component in the imprinted materials, the magnetic MIS can be easy separated from the large volume of solution by applying an external magnet.

Reusability of M-MIS **1** was investigated by performing six successive regeneration cycles with NA binding of M-MISs and M-NISs. The results showed that the rebinding efficiency of M-MIS **1** tend to decrease after regeneration process (Fig. 2.20). Up to 3 complete cycles of the M-MIS **1** can be used with no significant lost in NA binding efficiency. Unfortunately, after the forth regeneration, there the discrimination between M-MIS **1** and M-NIS was not observed indicating that there are no imprinting effect on these reused M-MIS **1**. The lost of rebinding efficiency was probably due to regeneration process by sonication in highly polar solvent causing a destruction of recognition site of M-MIS **1**.

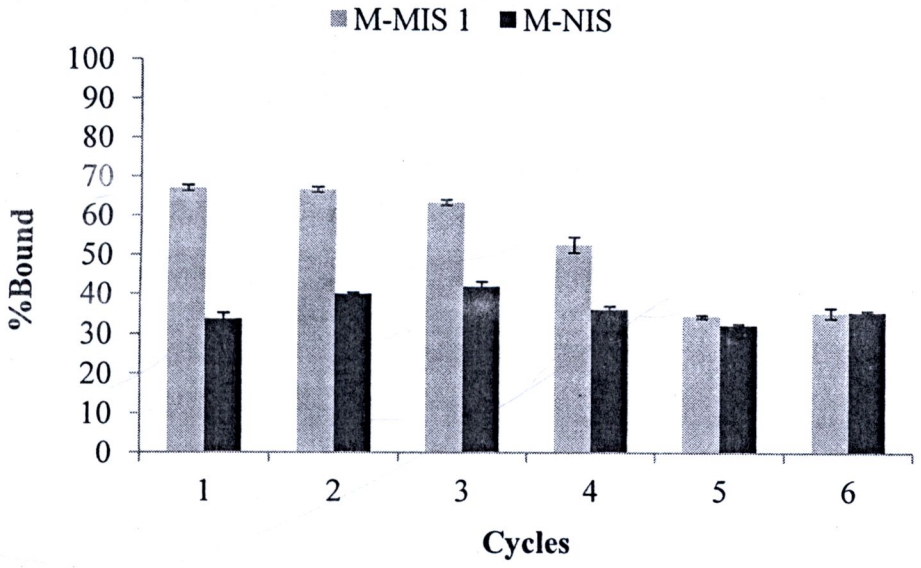


**Figure. 2.20** The binding efficiency of M-MIS **1** with the number of recycle times